



PROBABILISTIC CHARACTERIZATION OF OVERTURNING CAPACITY FOR SIMPLY-SUPPORTED RIGID BLOCKS

Elia VOYAGAKI¹ and Dimitrios VAMVATSIKOS²

ABSTRACT

A probabilistic treatment to the problem of rocking and overturning of a simply-supported rigid block is presented in the context of Performance-Based Earthquake Engineering (PBEE). To this end, a two-dimensional rectangular block resting at ground surface on a rough, horizontal, tensionless and cohesionless rigid base is considered, subjected to a suite of 44 horizontal earthquake excitations. The roughness of the interface is assumed to be sufficiently large so that sliding is prevented, while the flexibility of the block and aerodynamic effects are neglected. Rocking response curves are calculated for increasing ground motion intensity (or decreasing uplift strength) via Incremental Dynamic Analysis (IDA), and results are summarized in the form of 16%, 50% and 84% fractile IDA curves. The solution based on a geometrically linearized rocking equation is advantageous, as it limits the problem parameters to just three that is, uplift “yield” strength, pseudo natural frequency and coefficient of restitution (damping), as in the classical yielding oscillator. On the other hand, the slenderness angle of the block is not an essential independent variable, as it simply normalizes the response angle. Generalized overturning criteria are proposed covering a wide set of excitations and block parameters. By employing non-linear regression analysis, simple formulae are developed for both the median/mean and the dispersion of response to provide a complete probabilistic characterization of rocking response for use in PBEE.

INTRODUCTION

Starting with the seminal publication of Housner (1963), the rocking response of un-deformable free standing blocks to earthquake ground shaking has attracted the attention of several researchers. Despite its apparent simplicity, the problem is difficult to treat analytically, as determining the response can be challenging even for the simplest waveforms due to inherent nonlinearity and presence of transcendental functions. Only a handful of cases have been solved completely, mostly for pulses of half-cycle duration (Housner 1964, Shi et al. 1996, Voyagaki et al. 2013), whereas for full-cycle pulses analytical solutions leading to exact or approximate overturning criteria are even fewer (Dimitrakopoulos and DeJong 2012, Voyagaki et al. 2014). Extending the overturning criteria to actual ground motions is difficult, as the survival or toppling of a block depends on the details of excitation (Yim et al. 1980, Ishiyama 1982, Psycharis and Jennings 1983, Spanos and Koh 1984). In this light, a pertinent probabilistic treatment of the problem appears desirable.

In this work, the problem is treated numerically in the realm of two-dimensional rigid-body dynamics, with the results post-processed from a probabilistic viewpoint to provide simple response criteria applicable to a wide range of far-field earthquake motions. The methodology of Incremental Dynamic Analysis (Vamvatsikos and Cornell 2002, 2004) is employed to this end. The

¹ Post-Doctoral Researcher, J.B. ATE, Heraklion, Greece, eliavoyager@hotmail.com

² Lecturer, National Technical University of Athens, Athens, Greece, divamva@central.ntua.gr

forementioned analytical investigations for simple pulses (Housner 1963, Voyagaki et al. 2013, 2014) provided the fundamental means for casting light into several complex trends observed in numerical and experimental studies, including the effects on overturning of block slenderness, size, amplitude of base excitation and coefficient of restitution. Non-linear regression analyses provided the means for developing simple parametric equations that offer a complete probabilistic characterization of rocking response for use in Performance-Based Earthquake Engineering (PBEE).

PROBLEM DEFINITION

The problem under investigation concerns rocking of a rigid block resting on a horizontal rough rigid plane, subjected to a suite of earthquake motions acting parallel to the plane (Fig.1a). The block is of rectangular shape having mass m , dimensions $(2 \times b)$ by $(2 \times h)$ – leading to a radial distance from the center of rotation to the center of gravity $R = (b^2 + h^2)^{1/2}$ and a dimensionless slenderness angle $\alpha = \tan^{-1}(b/h)$. The friction coefficient at the interface between block and base is assumed to be sufficiently large to prevent sliding, while the flexibility of the block and aerodynamic effects are neglected. The restoring force is shown in Fig.1b.

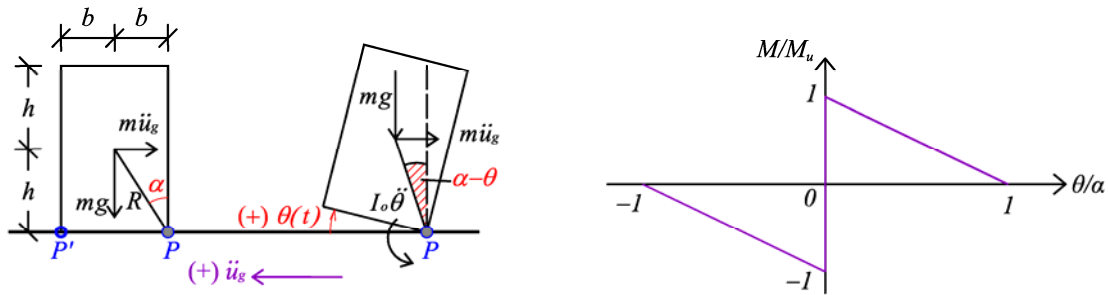


Figure 1. Rocking block on a rigid base and linearized resisting moment-rotation backbone curve in Eq.(2).

The non-linear equation governing rocking response of a rigid block is (Housner 1963)

$$I_o \ddot{\theta} + mgR \sin[\alpha - \theta \operatorname{sgn}(\theta)] \operatorname{sgn}(\theta) = +m\ddot{u}_g R \cos[\alpha - \theta \operatorname{sgn}(\theta)] \quad (1)$$

where I_o is the moment of inertia of the block with respect to its corner P or P' (for rectangular geometry, $I_o = 4mR^2/3$) and $\operatorname{sgn}(\cdot)$ denotes the signum function. The positive sign on the right-hand side of the equations is to ensure positive rocking response for positive ground acceleration, as evident from the reference system of Fig.1a.

For slender blocks angle α is small; the above equation can be linearized using the first-order approximations $\sin(\alpha \pm \theta) \cong \alpha \pm \theta$, $\cos(\alpha \pm \theta) \cong 1$ and re-written in the form:

$$\ddot{\theta} - p^2 \theta = +p^2 \ddot{u}_g / g - p^2 \alpha \operatorname{sgn}(\theta) \quad (2)$$

where $p = (3g/4R)^{1/2}$ is a measure of the dynamic characteristics of the block. Since the restoring force is exclusively due to gravity (as in the classical pendulum problem), the intrinsic frequency p is independent of the block mass. It should be noted that the second term on the right side of the equation refers to a constant restoring force in each response branch, whereas the second term on the left side can be interpreted as a negative (geometric) stiffness.

Assuming that sliding is prevented, initiation of rocking requires exceedance of the restoring moment due to self-weight, by the overturning moment due to inertia i.e., $m \cdot \ddot{u}_g \cdot h \geq m \cdot g \cdot b$. For slender blocks ($\alpha < 20$ degrees), this can be written as $\ddot{u}_g / g \geq \alpha$. The ratio of slenderness over dimensionless peak pulse acceleration ($\alpha g / A_g$), to be referred hereafter to as *uplift strength* η , has the following properties: if $\eta > 1$ no rocking occurs, if $\eta < 1$ rocking initiates at $t = t_{up}$, when $\ddot{u}_g(t_{up}) \cong \alpha g$.

According to the adopted notation (Fig.1), up to the point of impact the block rocks around the right edge (pivot point P) with positive uplift angles; after impact rocking continues around the left edge (pivot point P') with negative uplift angles. The transition from one pivot point to the other is accompanied by energy loss during impact, even for non-dissipative block and base materials. The reduction in kinetic energy during transition is $r = (\dot{\theta}_i^+ / \dot{\theta}_i^-)^2$, subscript i standing for ‘‘impact’’. Assuming perfectly inelastic impact (i.e., no bouncing) and using conservation of angular momentum, Housner (1963) evaluated r for slender rectangular blocks at $\varepsilon = \sqrt{r} = 1 - 3/2\alpha^2$, which defines the familiar coefficient of restitution. Clearly this is an upper-bound estimate, as the true coefficient of restitution is always smaller than the one disregarding bouncing.

Table 1. The forty-four ground motions of the FEMA P695 far field set (FEMA 2009).

No	Event	Date	M _w	Station	Closest Fault Distance (km)	Orientation	A _g (g)	V _g (cm/s)
1	Manjil, Iran	20/6/1990	7.4	Abbar	12.6	Long	0.515	42.5
2						Trans	0.496	52.1
3	Kocaeli, Turkey	17/08/1999	7.4	Arcelik	17.7	000	0.218	17.7
4						090	0.149	39.5
5	Friuli, Italy	06/05/1976	6.5	Tolmezzo	37.7	000	0.351	22
6						270	0.315	30.8
7	Superstition Hills, CA	24/11/1987	6.7	El Centro Imp.Co. Center	13.9	000	0.358	46.4
8						090	0.258	40.9
9	Duzce, Turkey	12/11/1999	7.1	Bolu	17.6	000	0.728	56.4
10						090	0.822	62.1
11	Superstition Hills, CA	24/11/1984	6.7	Poe Road	12.4	270	0.446	35.7
12						360	0.30	32.8
13	Loma Prieta, CA	18/10/1989	6.9	Capitola	14.5	000	0.529	36.5
14						090	0.443	29.3
15	Chi-Chi, Taiwan	20/09/1999	7.6	CHY101	11.1	W	0.353	70.6
16						N	0.440	115
17	Landers, CA	23/07/1992	7.3	Coolwater	21.2	Long	0.283	25.6
18						Trans	0.417	42.3
19	Kocaeli, Turkey	17/08/1999	7.4	Duzce	12.7	180	0.312	58.8
20						270	0.358	46.4
21	Loma Prieta	18/10/1989	6.9	Gilroy Array #3	14.4	000	0.555	35.7
22						090	0.367	44.7
23	Imperial Valley, CA	15/10/1979	6.5	Delta	43.6	262	0.238	26
24						352	0.351	33
25	Imperial Valley, CA	15/10/1979	6.5	El Centro Array # 11	12.6	140	0.364	34.5
26						230	0.380	42.1
27	Hector Mine, CA	16/10/1999	7.1	Hector	11.7	000	0.266	28.6
28						090	0.337	41.7
29	Northridge, CA	17/01/1994	6.7	Canyon County – W Lost Canyon	13	000	0.410	43
30						270	0.482	45.1
31	Northridge, CA	17/01/1994	6.7	Beverly Hills – 14145 Mulholland	19.6	009	0.416	59
32						279	0.517	62.8
33	Kobe, Japan	16/01/1995	6.9	Nishi – Akashi	11.1	000	0.509	37.3
34						090	0.503	36.6
35	San Fernando, CA	09/02/1971	6.6	LA Hollywood Stor Lot	21.2	090	0.210	18.9
36						180	0.174	14.9
37	Cape Mendocino, CA	25/04/1992	7.1	Rio Dell Overpass	18.5	270	0.385	43.9
38						360	0.549	42.1
39	Kobe, Japan	16/01/1995	6.9	Shin-Osaka	15.5	000	0.243	37.8
40						090	0.212	27.9
41	Chi-Chi, Taiwan	20/09/1999	7.6	TCU045	24.1	W	0.474	36.7
42						N	0.512	39
43	Landers, CA	28/06/1992	7.3	Yermo Fire Station	24.9	270	0.245	51.5
44						360	0.152	29.7

As far as the seismic excitation is concerned, the FEMA P695 (FEMA 2009) far-field ground motion set was selected for the analyses, comprising 22 pairs of strong acceleration time histories, (Table.1) that belong to a bin of relatively large magnitudes of 6.5 to 7.6 and bear the following characteristic attributes: average Joyner-Boore and Campbell source-to-site distance $>10km$; peak

ground acceleration $A_g > 0.2g$ and peak ground velocity $V_g > 15 \text{ cm/sec}$; $V_{s,30} > 180 \text{ m/s}$ (all selected records correspond to C/D NEHRP sites); limit of 6 records from a single seismic event; lowest useable frequency $< 0.25 \text{ Hz}$, to ensure that the low frequency content has not been removed by the ground motion filtering process; strike-slip and thrust faults; no consideration of spectral shape.

Summarizing, the problem parameters can be reduced to five: Block size or characteristic frequency, described by p in units of (1/Time), damping or energy dissipation during impact, described by the coefficient of restitution ε , block slenderness α , an intensity measure selected here to equal peak ground acceleration A_g , and the predominant period of the excitation, $2 \cdot t_d$. Assuming a slender block, the number of parameters is further reduced to three dimensionless quantities, ε , $f = p \cdot t_d$ expressing the size of the block or the frequency content of the excitation, and $\eta = \alpha \times g / A_g$, which expresses the resistance of the system to uplift and varies in the range $[0, 1]$: $\eta = 0$ refers to an infinitely slender block with zero resistance to uplift or an infinitely large peak ground acceleration, while for $\eta > 1$ the peak ground acceleration does not suffice to initiate rocking.

ANALYTICAL SOLUTIONS

The analytical solutions for simple pulse waveforms provided the initiative for this work as they cast light into the physics of this complex problem and help us understand the key characteristics of the response. More importantly, they can be extended in the realm of probability to apply to general problems and provide general overturning criteria for design purposes. To this end, a brief review of the available closed-form solutions is presented.

Until recently, the only available closed-form analytical solutions describing conditions of overturning, concerned the rocking response to half-cycle pulses of rectangular (Housner 1963) and sinusoidal shape (Shi et al. 1996). The criterion for overturning under a half-cycle rectangular pulse is:

$$\eta < 1 - e^{-f} \quad (3)$$

where $\eta = \alpha g / A_g$ is the dimensionless uplift strength and $f = p t_d$ the dimensionless pulse duration, equal to the characteristic frequency of the block p in units (1/time) times the half-cycle pulse duration t_d .

An extensive set of exact overturning criteria has been recently published by Voyagaki et al. (2013, 2014) which are applicable to symmetric pulses of half- and full-cycle duration, described by a generalized waveform controlled by a single shape parameter β to cover the whole range from a perfect rectangle (“box”) to a perfect impulse (“spike”) as shown in Fig.2. For a half-cycle case

$$\ddot{u}_g(t) = \frac{A_g}{1 - e^\beta} [1 - e^{2\beta t/t_d} + (e^{2\beta t/t_d} - e^{2\beta(1-t/t_d)})H(t - t_d/2) - (1 - e^{2\beta(1-t/t_d)})H(t - t_d)] \quad (4)$$

where $H(\cdot)$ denotes the Heaviside (step) function.

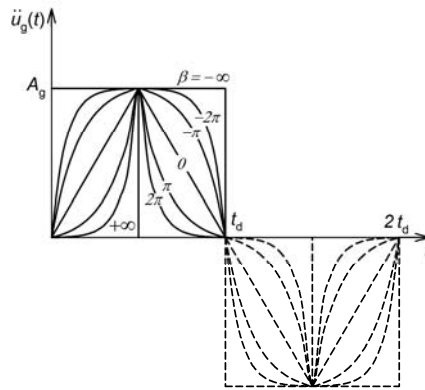


Figure 2. Ground acceleration time history for a generalized pulse (Eq.4).

The overturning criterion for the whole suite of half-cycle pulses at hand is expressed by the following closed-form expression

$$\eta_w = \frac{1}{1 - e^{-\beta}} \left\{ 1 - \left[\frac{e^f (f + 2\beta)}{2f e^{\frac{f}{2} + \beta} - (f - 2\beta)} \right]^{\frac{2\beta}{f - 2\beta}} \right\} \quad (5)$$

Considering the simple case of a rectangular pulse ($\beta \rightarrow -\infty$), Eq.(5) simplifies to the solution by Housner in Eq.(3). In the above equation η_w is interpreted as a limit strength separating systems that overturn ($\eta < \eta_w$) from those that do not ($\eta > \eta_w$). In this light, the curve $\eta_w = \eta_w(f, \beta)$ is referred in the ensuing to as “safety wall”.

The above solutions are presented graphically in Fig.3 which depicts the areas of safety and overturning as function of uplift strength η and pulse duration f for different values of the shape factor β , ranging from $-\infty$ (perfect rectangle) to $+\infty$ (perfect spike). Evidently, for large values of uplift strength overturning requires large pulse duration and vice versa.

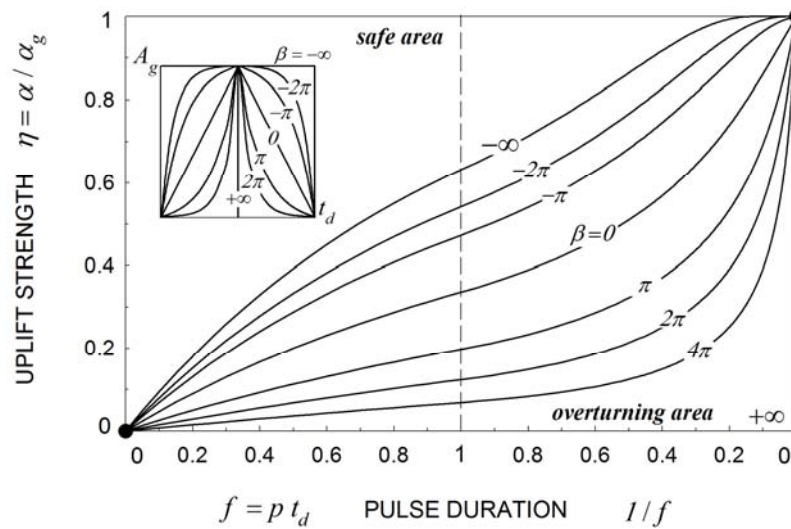


Figure 3. Areas of Safety (S) and Overturning (O) for a rocking block under an exponential pulse excitation of half-cycle duration for different values of shape factor β (Voyagaki et al. 2013).

Response to a full-cycle pulse is far more complicated than that to its half-cycle counterpart, as the existence of the second, negative, excitation lobe allows overturning of the block under two distinct, mutually exclusive modes: *Mode 0*, corresponding to overturning in the forward sense without impact; and *Mode 1*, that is overturning in the backward sense following a single impact and rocking reversal (Zhang and Makris 2001). The overturning criterion for *Mode 0* in f - η space in the simplest case of a full-cycle rectangular pulse is defined as

$$\eta_w = (1 - e^{-f})^2 \quad (6)$$

and will be proven particularly useful in describing critical strength to actual earthquake excitations as explained later in the paper. Criteria for overturning after an impact (*Mode 1*) are far more complicated (Voyagaki et al. 2014) and lie beyond the scope of this study. Fig.4 depicts the limits of the two modes including the effect of the coefficient of restitution on *Mode 1*. It will be shown that the mathematical description of the curves corresponding to the specific mode of overturning are not particularly important for actual earthquake ground motions. On the other hand the effect of the coefficient of restitution is significant.

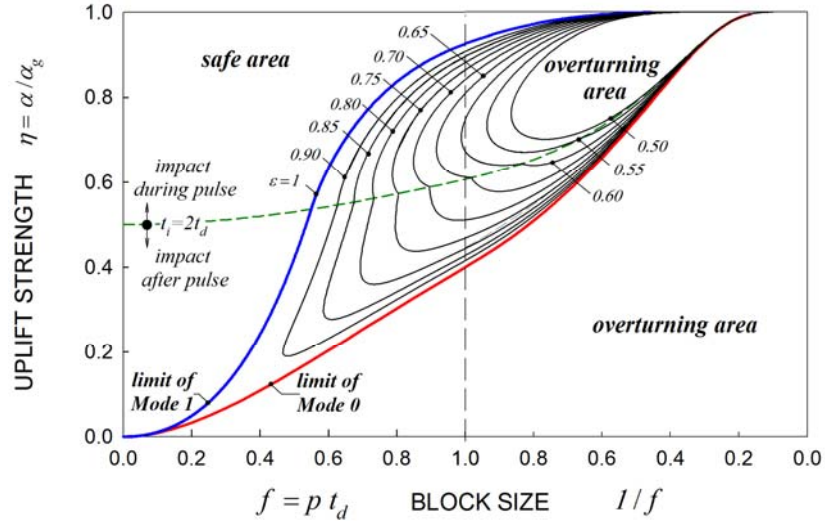


Figure 4. Areas of overturning without an impact (*Mode 0*), after one impact (*Mode 1*), and effect of the coefficient of restitution ε , for a rocking block under a symmetric rectangular pulse of full – cycle duration (modified after Voyagaki et al. 2014).

NUMERICAL SIMULATIONS

For performing the numerical analyses, a Matlab code was developed, capable of solving by a varying-order Runge-Kutta procedure the nonlinear equations of rocking motion in a continuous manner for an arbitrary excitation time history. Following the original proposal by Prieto et al. (2004), a compact formulation was derived to incorporate nonlinearities stemming from: (1) the transition from one rotation pivot point to the other; (2) the energy dissipation during impact and the associated discontinuity in angular velocity; and (3) the geometric nonlinearities expressed by the trigonometric terms in Eq.(1). The equation can be written in dimensionless form as

$$\ddot{x} + \frac{f^2}{\alpha} \operatorname{sgn}(x) \sin[\alpha(1 - x \operatorname{sgn}(x))] = \frac{f^2}{\eta} \cos[\alpha(1 - x \operatorname{sgn}(x))] \ddot{\psi}(\tau) + \ln(\varepsilon) \dot{x}^2 \delta(x) \operatorname{sgn}(\dot{x}) \quad (7)$$

where $x = \theta/\alpha$ denotes the normalized rocking angle, $\ddot{\psi}(\tau) = \ddot{u}_g(\tau)/A_g$ the acceleration-normalized earthquake waveform, $f = p t_d$, and $\tau = t/t_d$ dimensionless time. In the special case of a slender block, Eq.(7) simplifies to

$$\ddot{x} - f^2 x + f^2 \operatorname{sgn}(x) = \frac{f^2}{\eta} \ddot{\psi}(\tau) + \ln(\varepsilon) \dot{x}^2 \delta(x) \operatorname{sgn}(\dot{x}) \quad (8)$$

In light of Eq.(8), it is evident that the problem parameters have been reduced to three: ε , f and η . As for the suite of far-field motions at hand a unique predominant period t_d is hard to identify, the effect of record frequency content has been ignored and p is used in the ensuing as a parameter indicative of block size. This is tantamount to using $t_d = 1s$ in Eqs (7) and (8).

PROBABILISTIC APPROACH

For the suite of 44 earthquake motions of Table.1, the response was evaluated considering ten values of the restitution coefficient ε in the range (0.5-0.95) and twelve block radii ($\sim 0.07 - 70m$) corresponding to characteristic frequencies p in the range (0.33 – $10s^{-1}$). This leads to 120 parameter combinations per record. Applying the methodology of incremental dynamic analysis and selecting

peak ground acceleration as the intensity measure IM and peak rocking angle as the engineering demand parameter EDP, each record was scaled to cover the entire range of rocking response, from uplift, to rocking, to overturning. The peak rocking angles were evaluated for each motion that, in turn, was scaled by gradually increasing its acceleration amplitude so that overturning was encountered under all seismic records. To ensure the desired accuracy, 100 to 300 increments for each case were required depending on system characteristics. Considering an average of 200 increments per record, the total number of analyses exceeds 1 million (120x200x44).

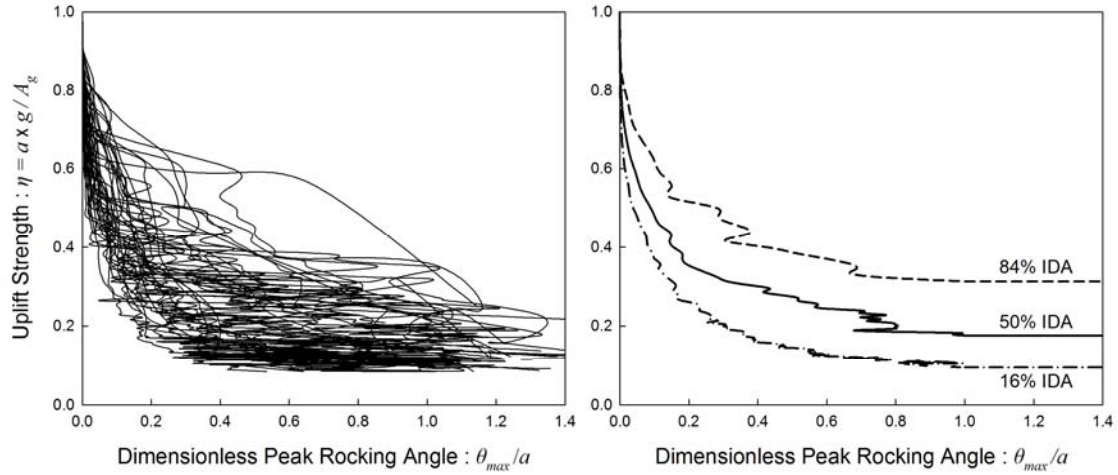


Figure 5. All forty-four IDA curves and their summary into their 16%, 50% and 84% fractiles for a given characteristic frequency $p=2s^{-1}$ and coefficient of restitution $\varepsilon=0.70$.

An example of the resulting IDA curve's for the whole suite of records and a given pair of ε , p , is provided in Fig.5a. The results are presented in dimensionless form, normalized by the block slenderness angle α . The IM is thus represented by uplift strength η and the EDP by the ratio θ_{max}/α . The horizontal flatlines reached by each curve for large levels of intensity indicate that overturning has occurred and thus provide critical levels of intensity (and strength) capacity: IM_c or η_c . Given that rocking is a problem of instability, attempting to determine a critical value of response, EDP_c becomes an ill-posed condition of lesser significance. In fact, any sufficiently large value of response practically corresponds to the same level of IM_c . Thus, mainly for reasons of visualization, the static overturning criterion $(\theta_{max}/\alpha)_c=1$ is selected as such an acceptable EDP_c . It could be similarly set to be "infinite" without any appreciable effect on the results (see Fig.5). Particular attention should also be paid to the phenomenon of "structural resurrection" (Vamvatsikos and Cornell, 2002) that may occur for some ground motion records: Due to each point on an IDA curve corresponding to a single (and independent) timehistory analysis, it may sometimes happen that a system will display multiple potential flatlines, seemingly coming back from global dynamic instability to display finite EDP response at an even higher value of IM. IM_c is then taken equal to the uplift strength that corresponds to the lowest such flatline, or equivalently, the first occurrence of overturning.

The IDA curves display a wide range of behaviors, showing large record-to-record variability, thus making it essential to summarize such data and quantify the randomness introduced by the waveforms. To this end, we need to employ appropriate summarization techniques that will reduce this data to the distribution of EDP given IM and to the probability of exceeding any specific limit-state given the IM level. This is achieved by calculating the 16%, 50%, and 84% fractile values of EDP for given IM levels. The 50% value (i.e., the median) is indicative of the central tendency, while the 16/84% percentiles represent the dispersion as illustrated in Fig.5b.

The effect of block size, measured through the characteristic frequency p , is shown in Fig.6, where the 16%, 50% and 84% IDA's are plotted for a given value of the coefficient of restitution. The safety wall, in full analogy to the notion presented in the analytical solutions, separates the systems that overturn from the ones that return to stability. As evident from the graphs, the larger the value of the characteristic frequency (or, equivalently, the smaller the size of the block), the easier it is for

overturning to occur. Conversely, the larger the size of the block the higher the ground motion intensity required to topple the block. This is in agreement with the findings of the analytical investigations based on the idealized half-cycle waveforms and further investigations on near-source pulsive earthquakes.

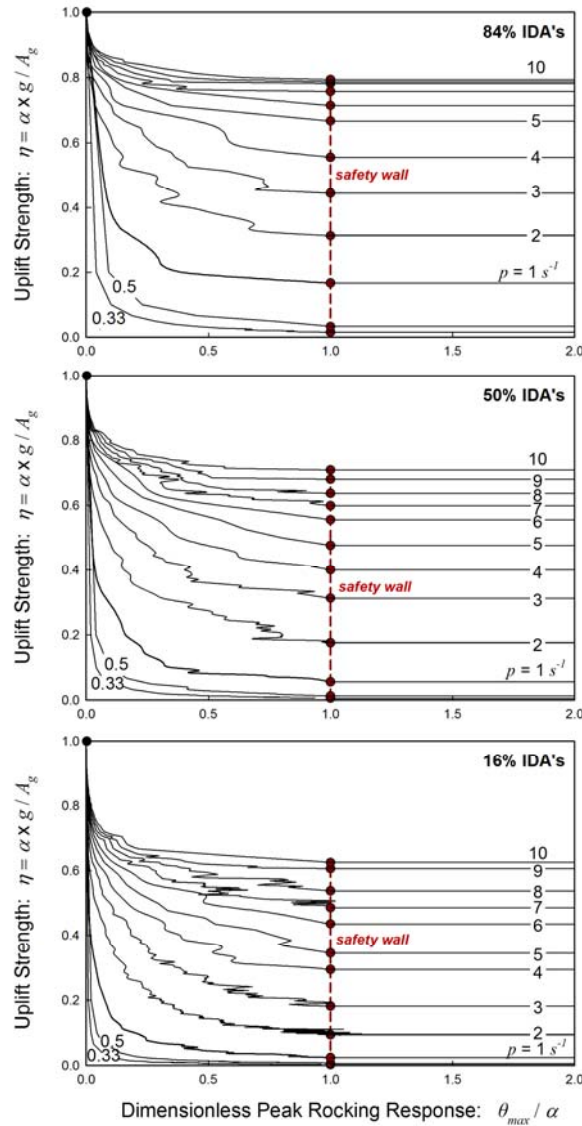


Figure 6. Comparison of 16%, median and 84% IDAs as function of the characteristic frequency p , for the suite of 44 far field motions in Table.1; $\varepsilon = 0.70$.

When summarizing the IDA curves, one may use stripes of EDP given levels of IM (“horizontal statistics” with respect to Fig.5, thanks to Prof. H. Krawinkler), or stripes of IM given EDP (“vertical statistics”, similarly). The issue whether one should summarize given IM or EDP has been extensively discussed in Vamvatsikos & Cornell (2004) and it has been shown that they are essentially equivalent representations when a sufficiently large number of ground motion records has been employed. Significant differences may appear when low numbers of ground motions are used, simply due to the frequent use of linear interpolation to determine the percentiles. For example, when having an even number of records, the median is estimated as the average of the two values closest to the middle of the sample. It is obvious that close to the flatline any summarization given EDP will always encounter finite values of IM, while summarization given IM will have to deal with “infinite” EDP responses. Since the average of a finite and an infinite (i.e., very large) value is always governed by the latter,

some differences are expected to appear. For the case at hand, a comparison of the two alternative approaches is presented in Fig.7. showing that 44 records are enough to remove any such issues. Nevertheless, it is always conceptually simpler to determine IM_c as the critical uplift strength η_c for a given $(\theta_{max}/\alpha)_c$ that is indicative of collapse (i.e. “infinite”), a value set to be 1.0 in our case. The ensemble of resulting values of overturning capacity thus estimated in terms of the percentile curves are grouped in Fig.8

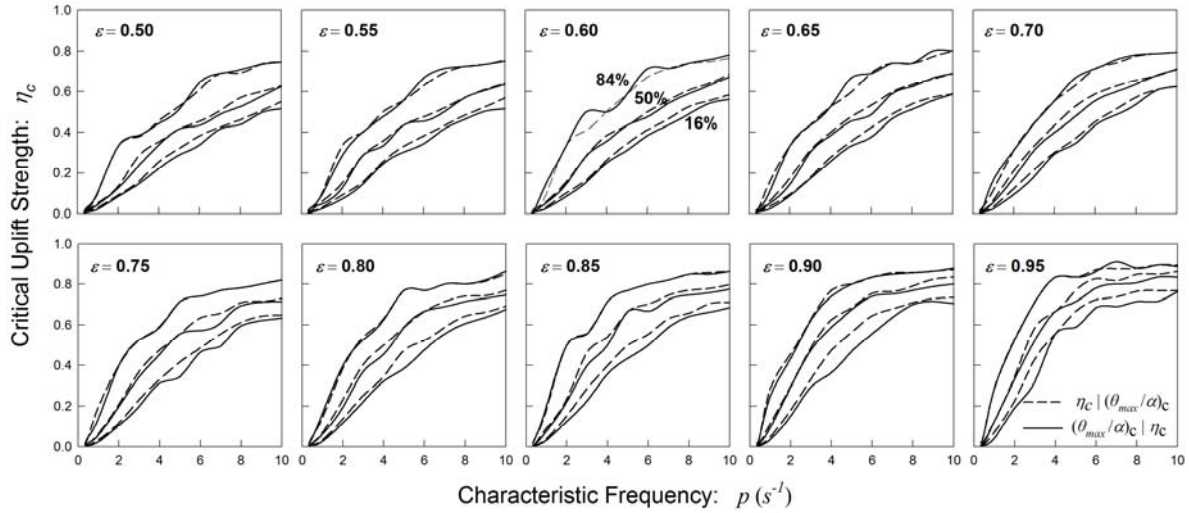


Figure 7. 16%, 50% and 84% percentiles of critical uplift strength as function of characteristic frequency, for different values of the coefficient of restitution. Critical strength values computed by summarization into fractiles of $\eta_c | (\theta_{max}/\alpha)_c$ (IM given EDP) versus fractiles of $(\theta_{max}/\alpha)_c | \eta_c$ (EDP given IM) are practically the same.

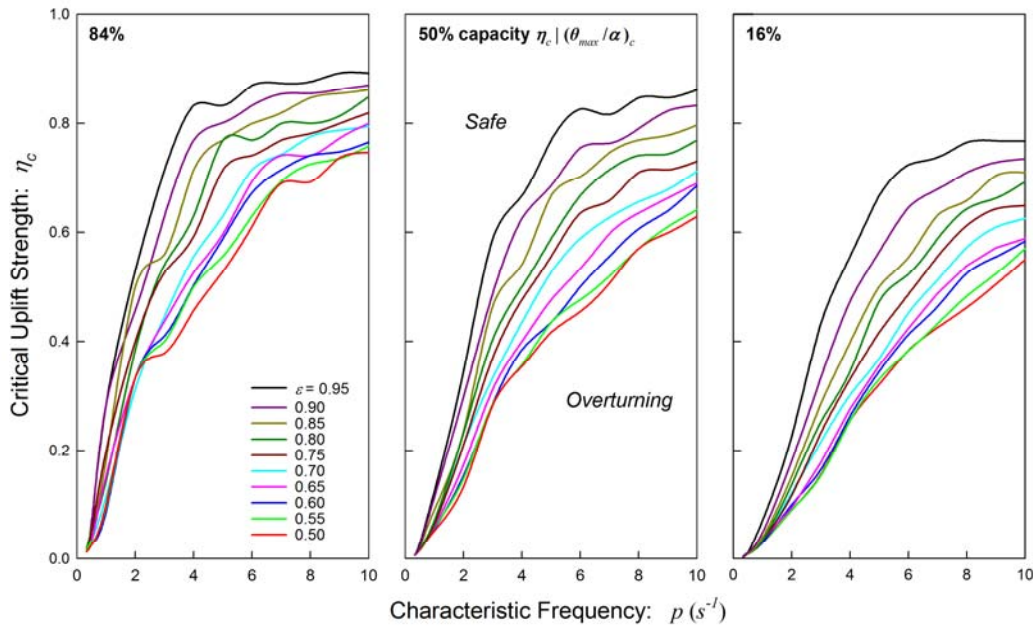


Figure 8. 16%, median and 84% capacity curves for the investigated systems.

Given that we are only evaluating three point estimates of the η_c distribution, i.e. the 16/50/84% values, it is important to establish an appropriate distribution model for the entire population. The lognormal assumption has been typically employed for the collapse capacity of yielding systems and it may also be appropriate for the distribution of overturning capacity. To this end, the Lilliefors test (Lilliefors 1967) was employed to test the (null) hypothesis that $\log(\eta_c)$ values come from a normally distributed population. The majority of the tests (about 80%) show that we do not have enough

evidence to reject this hypothesis at the 95% confidence level. The test p-values were generally higher than 10%. Thus, it may be stated in general that a lognormal distribution is an adequate model. Fig.9, provides two examples (out of 120 cases) of these distributions. Fig.9a is a typical example of cases with high p-values ($p_{val}>20\%$) and shows good agreement with the lognormal distribution assumption. Fig.9b refers to the non-conforming cases of very low p-values ($p_{val}<1\%$) where a right skew is apparent in the distribution. Better precision by means of additional increments in the area of calculated values of η_c seems to fix the problem.

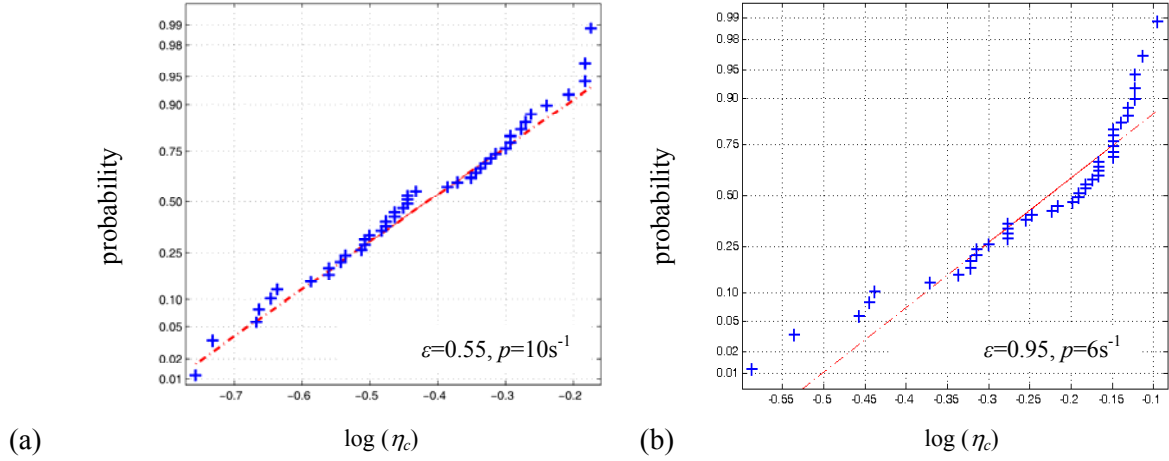


Figure 9. Lognormal probability plots of the overturning collapse capacity η_c . (a) $p_{val}=55\%$; (b) $p_{val}=0.3\%$.

Nonlinear Regression

A simple expression that describes a general overturning criterion, as function of the problem parameters η , p , ε , is desirable. To this end, the produced capacity curves were approximated by means of nonlinear regression. The existence of the analytical solutions made this task particularly easy as the regressions were based on the rigorous criterion for overturning under a full-cycle rectangular pulse given by Eq.(6). With that starting point we assumed that the critical uplift strength for the suite of motions at hand can be cast in the form

$$\eta_c = a(1 - e^{-bp})^c \quad (9)$$

where a , b , c are parameters depending on the coefficient of restitution ε . To achieve an estimate of η_c for different values of ε and p , a two-step regression was employed. First, coefficients a , b , c were fit via Eq.(9) for each given value of ε and each of the three different percentiles of η_c . Thus, for each percentile of η_c , three sets of a , b , c points versus ε were derived and subsequently fit by regression. For the median capacity they are described by the following first- and second-order polynomials shown in Fig.10

$$a_{50} = 0.44 + 0.43\varepsilon \quad (10a)$$

$$b_{50} = 0.56 - 1.14\varepsilon + 1.25\varepsilon^2 \quad (10b)$$

$$c_{50} = 1.66 - 0.38\varepsilon + 1.4\varepsilon^2 \quad (10c)$$

For dimensional conformity p , (measured in s^{-1}) in Eq.(9) should be multiplied by $t_d=1s$. Corresponding expressions were also produced for the 16% and 84% capacities:

$$a_{16} = 0.5 + 0.33\varepsilon \quad (11a)$$

$$b_{16} = 1.64 - 4.39\varepsilon + 3.44\varepsilon^2 \quad (11b)$$

$$c_{16} = 7.17 - 15.65\varepsilon + 12\varepsilon^2 \quad (11c)$$

and

$$a_{84} = 0.64 + 0.24\varepsilon \tag{12a}$$

$$b_{84} = -0.66 + 2.32\varepsilon - 0.94\varepsilon^2 \tag{12b}$$

$$c_{84} = -2.28 + 10.3\varepsilon - 6.27\varepsilon^2 \tag{12c}$$

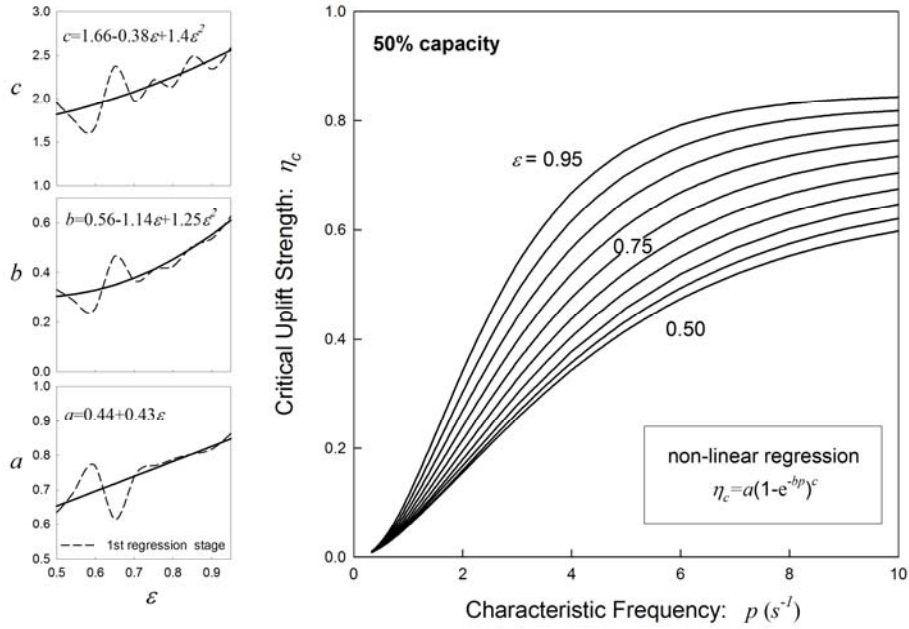


Figure 10. Median percentiles of critical uplift strength, calculated via nonlinear regression of the numerical data. The figures on the left represent the secondary fitting of the coefficients of Eq.(9) for different values of the coefficient of restitution.

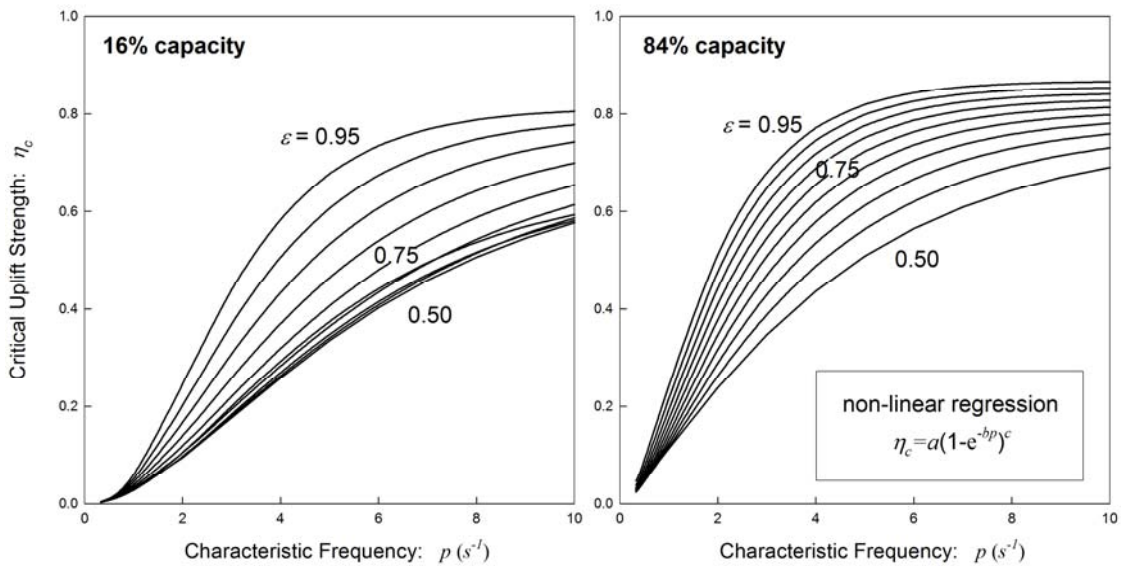


Figure 11. 16% and 84% percentiles of critical uplift strength, calculated via nonlinear regression of the numerical data; a, b, c from Eqs (11) & (12).

The approximate capacity curves represented by Eqs (9) – (12) are shown in Figs 10 and 11. As evident in Fig.11b the 16% capacity curves are not perfect at the lower values of ε , still, these are considered rather difficult to encounter. Further analyses will improve upon even that case.

CONCLUSIONS

The rocking behavior of a free-standing block resting on a rigid base and subject to 44 far-field earthquake motions was estimated numerically through Incremental Dynamic Analysis (IDA). Careful examination of the problem and the resulting data led to the following conclusions:

1. Overturning due to far-field seismic excitations may be reduced to three parameters: block size, expressed in terms of characteristic block frequency p , dimensionless uplift strength η [i.e., ratio of minimum required acceleration for initiation of uplift (or equivalently block slenderness angle) over peak ground acceleration] and coefficient of restitution ε .
2. The lognormal distribution is an adequate (although apparently imperfect) model for overturning capacity.
3. A simple expression based on closed-form solutions for the, so-called, safety wall can be exploited through non-linear regression techniques to provide a general probabilistic criterion for overturning under far-field ground motions.

The proposed expression allows for calculating both the median/mean and dispersion of response as a function of the coefficient of restitution and the characteristic frequency. The end result can be used to evaluate the probability of overturning for any rigid block resting on the ground, providing all the data needed for performance-based earthquake engineering applications.

ACKNOWLEDGEMENTS

This research has been co-financed by Greece and the European Union (European Social Funds) through the Operational Program “Human Resources Development” of the National Strategic Framework (NSRF) 2007-2013.

REFERENCES

- Dimitrakopoulos E, DeJong M (2012) “Revisiting the rocking block: closed-form solutions and similarity laws” *Proceedings of the Royal Society*. 468(2144): 2294-2318.
- FEMA (2009) “Quantification of Seismic Performance Factors”, FEMA P-695 Report, prepared by the Applied Technology Council for the Federal Emergency Management Agency, Washington, D.C.
- Housner GW (1963) “The behavior of inverted pendulum structures during earthquakes”, *BSSA*, 52(2): 404-417.
- Ishiyama Y. (1982) “Motion of rigid bodies and criteria for overturning by earthquake excitations”, *Earthquake Engineering and Structural Dynamics*, 10: 635-650.
- Lilliefors H. (1967) “On the Kolmogorov–Smirnov test for normality with mean and variance unknown”, *Journal of the American Statistical Association*, 62: 399–402.
- Prieto F, Lourenço PB, Oliveira CS. (2004) “Impulsive Dirac-delta forces in the rocking motion”, *Earthquake Engineering and Structural Dynamics*, 33(7): 839–857
- Psycharis IN, Jennings PC (1983) “Rocking of slender bodies allowed to uplift” *Earthquake Engineering and Structural Dynamics*, 11: 57-76.
- Shi B, Anooshehpour A, Zheng Y, Brune JN. (1996) “Rocking and overturning of precariously balanced rocks by earthquakes.” *BSSA*, 86 (5): 1364-1371.
- Spanos PD, Koh AS. (1984). “Rocking of rigid bodies due to harmonic shaking”, *Journal of Engineering Mechanics ASCE*, 110(11): 1627-1642.
- Vamvatsikos D and Cornell CA (2002) “Incremental Dynamic Analysis”, *Earthquake Engineering and Structural Dynamics*, 31(3):491-514
- Vamvatsikos D and Cornell CA (2004) “Applied Incremental Dynamic Analysis”, *Eq. Spectra*, 20(2): 523-553.
- Voyagaki E, Psycharis IN, Mylonakis G (2013) “Rocking Response and Overturning Criteria for Free Standing Rigid Blocks to Single – Lobe Pulses.” *Soil Dynamics & Earthquake Engineering*, 46: 85–95.
- Voyagaki E, Psycharis IN, Mylonakis G (2014) “Complex Response of a Rocking Block to a Full-Cycle Pulse” *Journal of Engineering Mechanics ASCE*, doi: 10.1061/(ASCE)EM.1943-7889.0000712
- Yim CS, Chopra AK, Penzien J (1980) “Rocking response of rigid bodies to earthquakes”, *Earthquake Engineering and Structural Dynamics*, 8: 565-587.
- Zhang J, Makris N (2001) “Rocking response of a free-standing blocks under cycloidal pulses” *Journal of Engineering Mechanics ASCE*. 127(5): 473-483.